Thin Solid Films 645 (2018) 320–325

Contents lists available at ScienceDirect

Thin Solid Films

journal homepage: www.elsevier.com/locate/tsf

Chemical vapor deposition - based synthesis of conductive polydopamine thin-films

Halime Coskun[a,*], Abdalaziz Aljabour[a], Lisa Uiberlacker[b], Moritz Strobel[b], Sabine Hild[b], Christoph Cobet[c], Dominik Farka[a], Philipp Stadler[a], Niyazi Serdar Sariciftci[a]

[a] Linz Institute for Organic Solar Cells (LIOS) and Institute of Physical Chemistry, Johannes Kepler University Linz, Altenbergerstraße 69, 4040 Linz, Austria
[b] Institute of Polymer Science, Johannes Kepler University Linz, Altenbergerstraße 69, 4040 Linz, Austria
[c] Center for Surface and Nanoanalytics, Johannes Kepler University Linz, Altenbergerstraße 69, 4040 Linz, Austria

ARTICLE INFO

Keywords:
Polydopamine
Thin film
Chemical vapor deposition
Conjugated bio-inspired material

ABSTRACT

Polydopamine (PDA) represents a family of synthetic bio-inspired pigments offering high functional activity combined with semiconducting properties. To date, it represents one of the main synthetic biopolymers used mainly because of its simple synthesis in aqueous solutions. Thereby dopamine polymerizes in the presence of ambient oxygen to polydopamine. However, its structure renders a sophisticated backbone relating to variations of ambient growth parameters such as temperature, local pH and partial oxygen pressure; preponderant repeating units found in aqueous polydopamine are 5,6-hydroxyl-indole derivatives. However, hydrogen-bonded aggregation competes with the polymerization leading to complex systems. In order to reduce the aggregation we hypothesized that acidic oxidants will direct the polymerization towards C—C coupling and hence create synthetic biopolymers.

In this work we demonstrate oxidative chemical vapor deposition (o-CVD) for PDA, where we obtain the desired consistent biopolymer thin-films as shown by structural analysis. Furthermore, as-gained polydopamine is conductive and renders fingerprint signatures of free charge carriers. Concomitantly it preserves its functionality – imperative for potential applications in catalysis or as bio-linker.

1. Introduction

Natural molecular units, such as hydrogen-bonded pigment molecules, represent an emerging class of conjugated semiconductors proposed for manifold bio-compatible optoelectronic linkers. Bio-compatible semiconductors can be implemented in living tissue and mutually address biologic-electronic signals. In addition, decomposable, non-toxic semiconductors can decrease electronic littering [1–7].

Among other bio-related conjugated systems polydopamines (PDAs) are commonly used conjugated biopolymers. PDAs adopt indole-based conjugated - functional repeating units reminiscent to eumelanins – a group of natural pigments built from 5,6-dihydroxy-indoles and derivatives thereof (Fig. 1). Unlike eumelanins, PDAs assemble to 1 - dimensional structures. Originally, they have been derived from 3,4-dihydroxy-L-phenylalanine – a protein existing in mussels responsible for the high binding strength. Consequently, early research has focused bio-mechanical applications [8–15]. Meanwhile the synthesis procedures have eased and PDAs are used in manifold coatings, template layers and catalyst carriers [15]. The dominant synthesis to date uses oxidative polymerization of dopamine in aqueous solutions [7,15–18]. Thereby, ambient oxygen serves as C—C coupling agent making the synthesis straightforward (*i.e.* self-polymerization in a glass beaker). However, the downside of aqueous synthesis is resulting complex structures such as disrupted conjugation. Studies have shown that entire building blocks of hydrogen bond networks (H-aggregates) are formed within PDA and inhibit covalent coupling among the monomers. Hence, aqueous PDAs are often not processable and show limited electronic properties [7,8,15]. In addition, the establishment of consistent growth parameters (*i.e.* temperature, pressure, local pH) is difficult, as minor changes in ambient conditions significantly alter the final molecular structure [8,9,15,19]. In order to promote covalent polymerization, monomer intermediate formation has to occur under controlled oxidative conditions. Discretely, these are the oxidation of dopamine (DA) to dopamine-quinone (DAQ), the intramolecular cyclization to leucodopaminechrome (LDC) and thereafter the formation and polymerization of indole and its derivatives (Fig.1) [15].

To suppress PDA's affinity to build up H-aggregates, we pursue a synthesis strategy that adopts insights from classic conductive polymers

* Corresponding author.
E-mail address: halime.coskun_aljabour@jku.at (H. Coskun).

https://doi.org/10.1016/j.tsf.2017.10.063
Received 2 August 2017; Received in revised form 19 October 2017; Accepted 31 October 2017

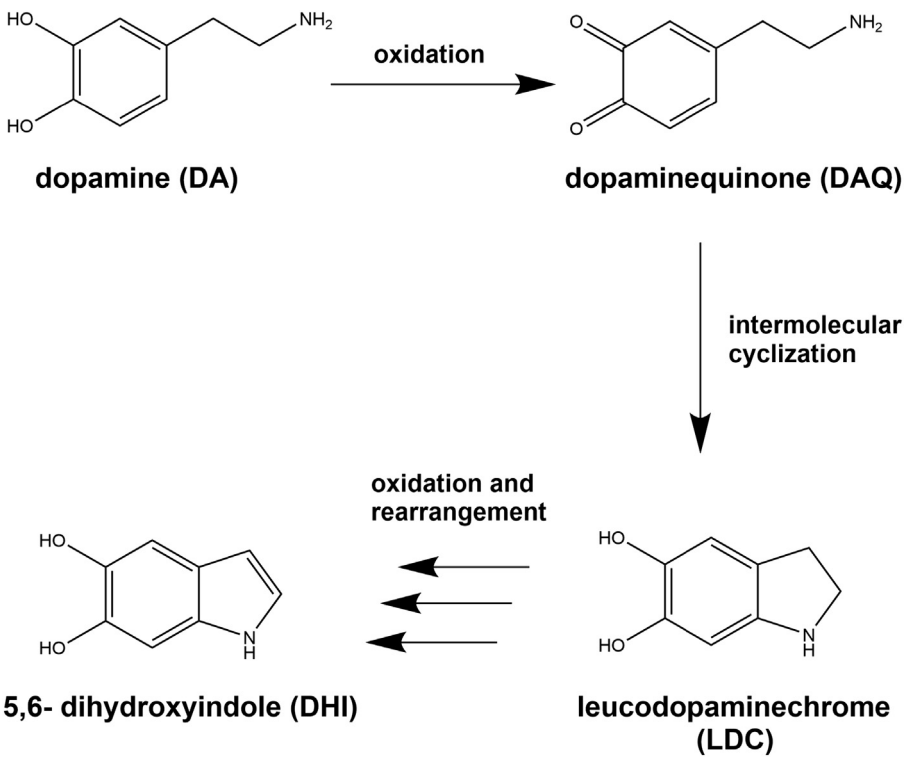

Fig. 1. Chemical structures of the polydopamine (PDA) intermediate steps undergoing numerous oxidation and rearrangement reactions.

[8,15,20]. The aim is to generate conjugated *and* conductive PDA from dopamine by using oxidative chemical vapor deposition (o-CVD). This technique allows us to use stronger oxidation reagent (as compared to ambient O_2) in combination with acidic surrounding to enforce oxidative C—C coupling. The goal is to arrive at the desired functionalized polyparaphenylene (PPP) type of backbone.

In this work we adapt o-CVD for PDA *i.e.* we contact gaseous dopamine free base with sulphuric acid. The latter serves as acidic oxidation agent and directs the synthesis to deposit conjugated and conductive PDA thin films; we can define film thickness and deposition on various substrates such as glass, sapphire or carbon-materials for potential (catalytic) applications [21]. We are in particular interested in the consequent structural changes induced by o-CVD (as compared to the aqueous PDA). Therefore, we employ spectroscopic tools such as Fourier Transform Infrared Spectroscopy (FTIR), Raman and variable angle spectroscopic ellipsometry (VASE) on par with structural investigations (atomic force microscopy - AFM). We find evidence of covalent polymerization and high structural consistency in o-CVD PDA on par with a preservation of its functionalization. O-CVD PDA offers higher processability and yields consistent structural conformity leading to electronic activations such as electrical conductivity.

2. Experimental detail

2.1. Materials and methods

The oxidative chemical vapor deposition (o-CVD) is conducted on glass substrates (20 mm × 20 mm) and sapphire (10 mm × 10 mm × 0.5 mm) purchased from CrysTecKristall technology with Cr/Au electrodes used for the characterization of the polymer films. For the conductivity measurements on sapphire, the metal contacts are deposited by PVD through a 4-in-line contact mask. First, the substrates are cleaned using ultra-sonic bath 15 min each in acetone, isopropyl alcohol, Hellmanex-detergent (Hellma, 70 °C) and deionized water. Before starting the synthesis, dopamine hydrochloride (Sigma Aldrich) is dried in an oven at 150 °C overnight in presence of CaH_2 (95%, Sigma Aldrich) to remove any water residual. The reaction is carried out in a tube furnace (Carbolite company; glass tube length: 45 cm; tube diameter: 2.4 cm; reaction temperature: 300 °C) under nitrogen atmosphere with a carrier gas-flow of 3 L/min. Sulphuric acid (95–97%, J.T. Baker) and sodium sulphate (≥ 99.0%, Sigma Aldrich) are utilized as oxidation agent and corresponding salt in the synthesis, respectively, in order to shift the balance towards SO_3^- and SO_4^{2-} in the gas phase. The reaction times are varied to reach the desired film thickness. For electrical characterization the samples are stored under inert conditions to avoid humidity and are sealed by drop casting a polymethyl methacrylate (PMMA) film on top of the active area. The simplified structure of vapor phase polydopamine during the one-step polymerization in the tube furnace is presented in Fig. 2.

2.2. Film characterization

The FTIR measurements are done using a Bruker Vertex 80 (8000 cm^{-1} to 600 cm^{-1}; resolution 4 cm^{-1}). The Raman spectra are recorded at room temperature with a WITec Alpha 300 R-Raman-System (WITec GmbH, Ulm, Germany) instrument. Nd:YAG laser (532 nm) is used for the excitation and thermoelectrically cooled CCD (DU970N-BV) detector is applied for all measurements. A grating of 600 mm^{-1} is used with a resolution of 4 cm^{-1}. For all three molecules 20 × Zeiss EC Epiplan (Carl Zeiss Jena GmbH, Germany) objective lens is used, while the laser intensity, integration time and accumulations are varied for the monomer (10 mW, 15 s., 10), aqueous PDA (5 mW, 2 s., 3), and o-CVD PDA (5 mW, 3 s., 20), respectively.

Variable angle spectroscopic ellipsometry (VASE) measurements are conducted using a Wollam M-2000 spectrometer at 6 incident angles. The dielectric model has been derived using VASE program with film thickness used as an input parameter. For electrical characterization PMMA-sealed PDA films are contacted using indium solder and loaded to the cryosystem for electrical probing (Physical Property Measurement System, DynaCool, Quantum Design). The electrical conductivity is characterized as a function of temperature and time (at 300 K). The surface imaging of polydopamine films is taken by MFP 3D-Stand Alone atomic force microscopy (AFM) from Asylum Research with the cantilever OMCL-AC240TS of Olympus. It is operated in the

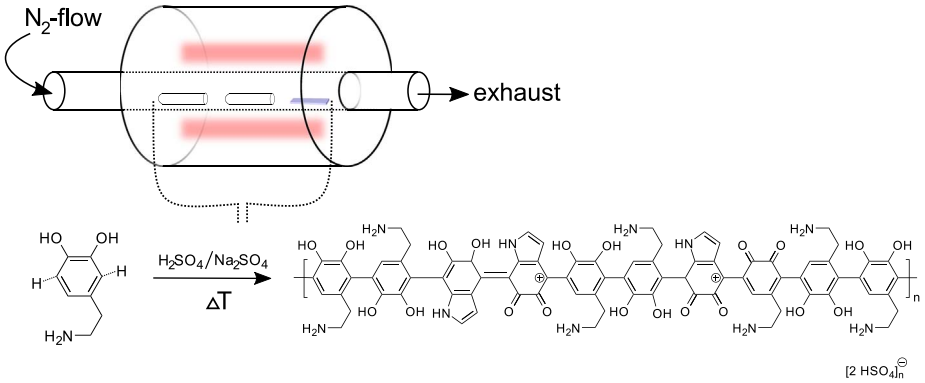

Fig. 2. Experimental setup of the o-CVD in the tube furnace. PDA is deposited on glass substrates in presence of the monomer and oxidation agent at an elevated reaction temperature of 300 °C under N_2 atmosphere. After the reaction the monomer is transformed into a doped conjugated polymer consisting of quinone and indole derivatives of dopamine.

AC-mode at 60% setpoint and a scan rate of 0.2 Hz. The thickness determination of the polymer films is carried on Bruker DektakXT.

3. Results and discussion

This work utilizes o-CVD to grow conductive PDAs. Prior art on state-of-the-art techniques uses mainly solution-based synthesis (Table 1) [18,22–25].

As discussed, the downside of solution-based synthesis is the difficulty of the control over ambient parameters (temperature, O_2 partial pressure, local pH in growth solution) and the competing H-aggregation disrupting conjugation. We pick one archetype solution route (according to ref. 21) and use it as a control experiment (further denoted as *solution-PDA*) for comparison to our o-CVD processed PDA (*o-CVD PDA*).

O-CVD induces a rapid growth of PDA (Fig. 3) – typical deposition rates are 5–6 nm per minute (within 4 h thin films with high homogeneity and controllable thickness can be deposited). We found that acidic reaction conditions protonate the dopamine free base and as such deactivate the competing H-bond aggregation and hence preserve the functionality (most dominantly on the amine). Furthermore, as typically for o-CVD we obtain a conducting biopolymer. The vapor oxidation includes also the shallow doping step in the polymerization and results in highly defined, reproducible deposits. We could demonstrate o-CVD on various substrates such as flat surfaces but also mesh-type or sponge-type electrodes, which are effectively covered with PDA through vapor infiltration.

To elucidate the surface topography of a glass-deposited PDA, we apply atomic force microscopy (AFM) (Fig. 4). The images reveal homogenously formed, pinhole-free surfaces with a root mean square roughness of 3 nm (obtained at 10 × 10 µm images on various spots). Similar morphologies at higher thickness in bulk-like films have been reproduced (not shown). The morphological consistency is also reflected in the optical properties.

In general, PDAs belong to the naturally occurring pigment family of eumelanin, consequently, the optical parameters of PDA are related to the natural chromophore [15]. These are characteristic broad band-monotonic absorbers in the ultraviolet. Exactly such absorption features

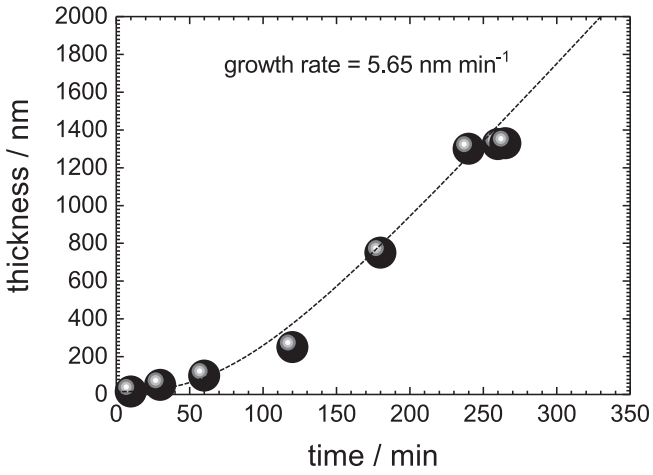

Fig. 3. Film thickness as a function of the deposition time after the o-CVD of PDA.

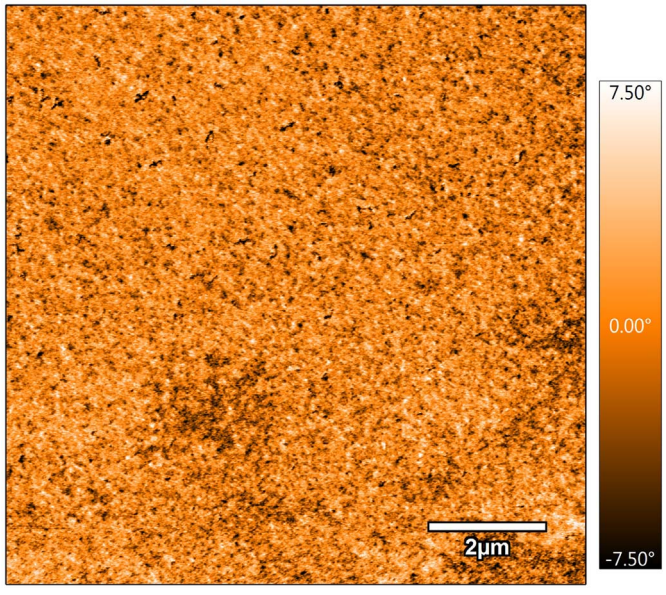

Fig. 4. Phase image of the film demonstrating a homogenous, pin-hole free surface. The film has a thickness of 1 µm.

Table 1
An overview about the recent status of the PDA deposition parameters.

Method of deposition	Oxidant	Deposition time [h]	Thickness [nm]	Ref.
Solution process	O_2	15	max. 40	[24]
Solution process	$CuSO_4$	80	< 80	[23]
Solution process	O_2	< 80	< 80	[18]
Solution process	O_2	< 30	< 80	[22]
Solution process	O_2	2–60 min	< 10	[25]
o-CVD	H_2SO_4/ Na_2SO_4	< 4	< 1500	This work

are found in o-CVD PDA as well – we derive the optical parameters using variable-angle spectroscopic ellipsometry to attain a profound insight (Fig. 5, relevant optical parameters as dielectric function ε_1 and ε_2). Furthermore, we derive the absorption coefficient α (Fig. 5a). Similar to eumelanin, an exponential increase is observed dominated in the UV region with the absorption peaks at 217 nm (5.71 eV), 238 nm

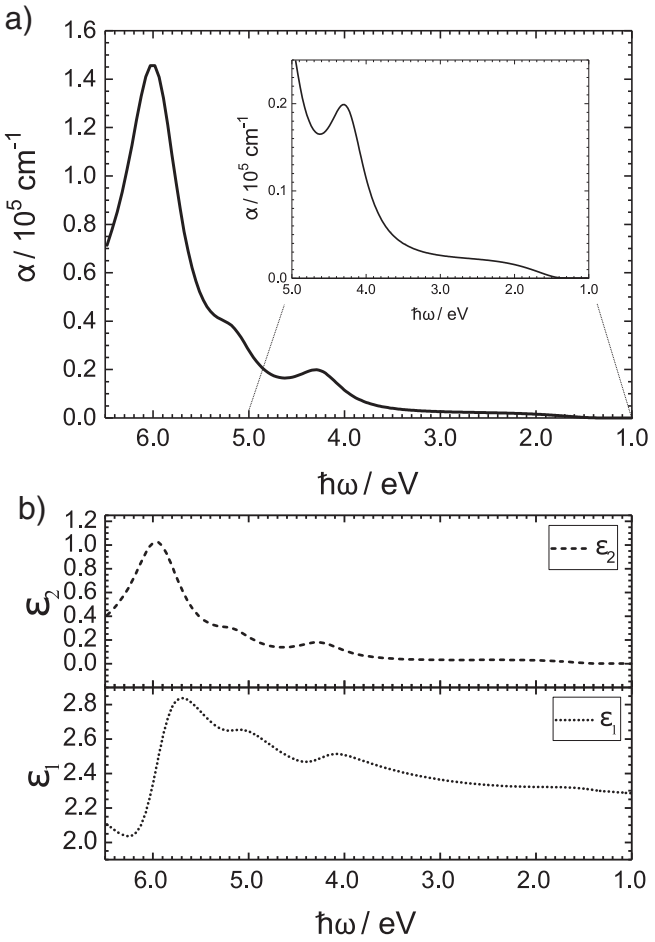

Fig. 5. (a) Absorption coefficient of o-CVD PDA (inset: zoom to the absorption onset). Two onsets are found. (b) Variable angle spectroscopic ellipsometry (VASE, 6 incident angles) on CVD-grown PDA thin films showing the dielectric function in the near-infrared, visible and UV spectral regime. We derive all optical parameters using a point-by-point fit. Note the functions are obtained by Kramers-Kronig relations.

(5.2 eV) and 300 nm (4.13 eV). We relate these strong absorption features to presence of leucodopaminechrome (LDC) and its indole derivatives reminiscent of the archetype UV-photoprotection of melanin skin pigments [15,26,27].

We conclude an absorption onset at approximately 3.72 eV – this is in agreement with previously reported theoretical calculations and experimental data on PDA. The optical dielectric parameters ε_1 and ε_2 of PDA have been derived using a chemical disorder models (CDM) [15]. Unlike classic conductive polymers alternating combinations of different monomers such as dopamine, LDCs including and its indole derivatives generate convoluted repeating units – CDM can bundle these complex variables and construct effectively broadened molecular orbitals. Consequently the UV-features (but also the corresponding near-IR features) are smeared out *i.e.* monotonic broadband features [15,28–30].

We use Raman and FTIR to expand CDM to the vibronic regime and to further elucidate the structural variety of o-CVD PDA. This allows us to explore a more detailed picture on the influence of discrete structural designs on the electronic properties - including the functional groups and complex IR-electronic features. Thereby we hypothesize that the functional sites are integrative part of the conjugated system thus leading to intimately structures functions-on-conjugation. To examine this entanglement in detail, we relate FTIR and Raman spectra attained from the actual monomer dopamine hydrochloride in comparison with o-CVD PDA and solution PDA (Figs. 6, 7 and 8).

Previous Raman studies have focused the identification of the

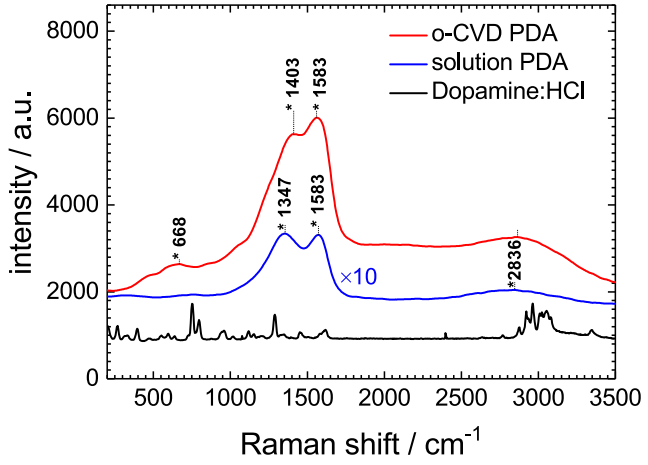

Fig. 6. Raman spectra of dopamine hydrochloride (black), solution PDA (blue, 10-fold expansion) and PDA synthesized by o-CVD (red). The signature peaks at 1403 cm^{-1} and 1583 cm^{-1} of o-CVD appear more intense in o-CVD PDA (as compared to solution PDA). Note 1403 cm^{-1} and 1583 cm^{-1} are aromatic C–N and C–C vibrations. (For interpretation of the references to colour in this figure legend, the reader is referred to the web version of this article.)

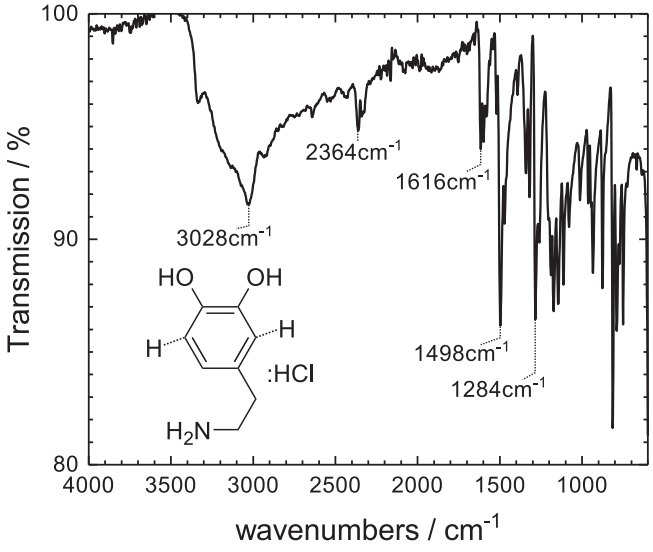

Fig. 7. The FTIR spectrum of dopamine hydrochloride (black).

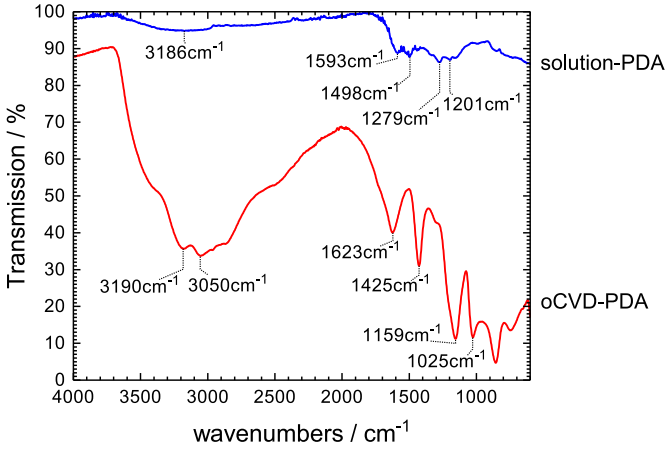

Fig. 8. The FTIR spectrum of solution processed PDA (blue) and PDA synthesized by o-CVD (red). (For interpretation of the references to colour in this figure legend, the reader is referred to the web version of this article.)

functional sites [31–33]. In this work we can use Raman to explore the distinct differences between solution and o-CVD PDA. In the monomer dopamine most pronounced peaks appear at 1616 cm^{-1}, 1455 cm^{-1}, 1349 cm^{-1} and 1287 cm^{-1} (first three assign the aromatic C—C stretching-, the last one aromatic C—H vibrations). In the polymer these peaks are changed - we observe three weak bands at 2836 cm^{-1}, 1583 cm^{-1} and 1347 cm^{-1} in solution-PDA. In o-CVD PDA, these bands are more intense (1583 cm^{-1} and 1403 cm^{-1}) – they refer to C—C vibrations of the aromatic units – hence we conclude that we actually surpass the H-aggregation towards effective C—C coupling in o-CVD PDA. Similarly, this effect is observed in the aromatic C—N bonds (Fig. 6) [31,32]. In o-CVD, weaker peaks at 2854 cm^{-1} and 668 cm^{-1} indicate suppressed aromatic O—H and the stretching and deformation of aromatic rings, respectively, again pointing at the increased C—C polymerization at cost of H-aggregation (Fig. 6).

Similar to Raman, also FTIR vibronic characterization reveals a strong interplay of hydrogen bonds triggering the formation of undesired broken conjugated networks from H-aggregation. We are interested to investigate the changes induced by o-CVD, in particular to explore if C—C coupling is distinct for the building of the desired functionalized polyparaphenylene (PPP) type of polymer backbone. Therefore, we separately plot the FTIR spectrum of dopamine hydrochloride as control (Fig. 7). Here, we see the broad and strong bands in the 3000–3400 cm^{-1} region hallmark signatures for intermolecular hydrogen bond oscillations on (aromatic) O—H stretching vibrations [10]. In comparison, the NH_2 functionality in the hydrochloride adduct moves to lower frequency, such as the N—H bands emerge between 2700 cm^{-1} and 2250 cm^{-1}. The intense peaks below 1700 cm^{-1} are attributed to aromatic C=C and C—H bonds.

When polymerized in solution (solution-PDA, blue line), the features between 3400 and 2954 cm^{-1} and 3000–2100 cm^{-1} remained resembling at blurry and weakened intensity corresponding to the aromatic O—H stretching vibrations region as well as the amine functionality patterns at 1593 cm^{-1} and 1498 cm^{-1}, respectively (Fig. 8) [9,10,34,35].

On the contrary, the spectrum of o-CVD PDA (red line) reveals almost united broad bands in the regions of 3000–3400 cm^{-1} and 2856–1623 cm^{-1}. We conclude that from the intensity, these features only partly render N—H or O—H vibrations, while the major oscillator corresponds to the broad polaron transition (maximum 3000 cm^{-1}). Moreover, the significant peaks between the 1660–1425 cm^{-1}relate to the conjugated, cyclic C=N group [10,34,35]. In parallel, strong carbonyl IR absorption bands are observed between 1590 and 1640 cm^{-1}, indicating the prevalent oxidation of the O—H functional groups to the corresponding ketones. Furthermore, the hallmarks of free charge carriers along the conjugated polymer chain are confirmed by the intense infrared-activated vibrations (IRAVs) in between 857 and 1075 cm^{-1} responsible for conductivity of the doped polymer films (as true for the polaron transition at 3000 cm^{-1}).

We denote that these fingerprint FTIR regime in o-CVD PDA is distinctively different to the solution PDA – peaks are by far more intense (we characterized similar amounts and the same setup) and, qualitatively, we clearly see IRAV, polaronic transitions and at the same time functional fingerprints such as cyclic C=N and carbonyl.

In order to confirm the free electron from shallow doping, we characterized the electrical conductivity of o-CVD PDA. Prior art in eumelanin-derived (hence PDA-related) structures has been explained conductivity resulting from protonic motion. Moreover, intrinsic polymer pigments such as UV-absorbing PDA are considered as amorphous and wide-bandgap organic semiconductors – both indications for high activation barriers to establish high mobility thus electrical conductivities. Hints of proton motion in eumelanin, however, gave the strong temperature dependence in presence of high humidity – the latter imperative ingredient to enable electrical transport: Without humidity, eumelanin and polydopamine show typically values across 10^{-13} S/m, while under humid atmosphere, these values increased up to 10^{-5} S/m (*e.g.* at 100% humid atmosphere) [15,36,37]. Especially, Meredith et al. proposed melanin in general to behave as electronic-ionic hybrid conductors with ionic motion responsible for transport [13]. Herein, we report a persistent and substantially higher conductivity of PDA films observed through the o-CVD in H_2SO_4. We achieve 0.4 S cm^{-1} at 300 K using 4-probe specimen (over a representative time scale and in inert conditions). Note that the temperature dependence reveals a steep rise according to Arrhenius type activation. Above 300 K, however, the transport mechanism is more complex (non-linear), thus we cannot exclude ionic contributions playing a more dominant role (Fig. 9).

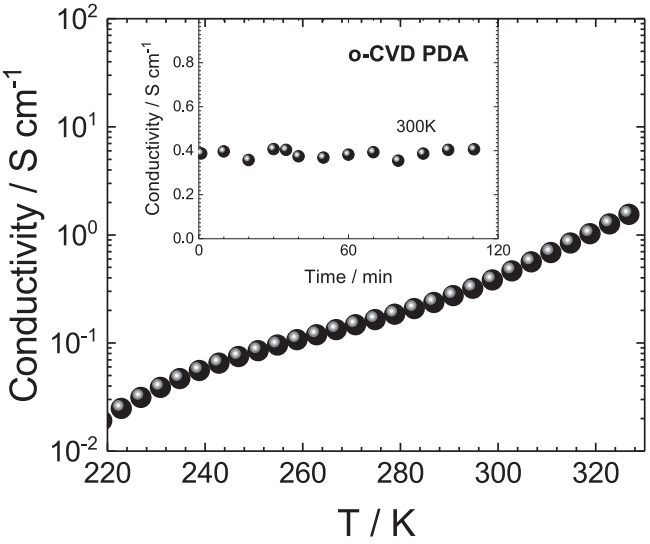

Fig. 9. Four probe conductivity measurement of o-CVD PDA films as a function of time (insert) and temperature.

We denote that we use controlled Helium atmosphere, while probing the current – leading us to the conclusion that the observed conductivity results predominantly from electrons rather than protonic/ionic movement.

The occurrence of electrical conductivity in PDA proves our strategy to utilize a stronger oxidant to improve the covalent path to form the desired chemical consistency *i.e.* the (functional) poly-paraphenylene. Obviously, the harsh conditions lead to further oxidation and as such include doping as in similar manner found for classic conducting polymers. The presence of free carriers is consequently evidenced by dc conductivity (actually 4 orders of magnitude higher than highest reported earlier for differently synthesized PDAs). We believe that represents a hallmark in biopolymers – a demonstration that tailoring synthesis can assist to implement bio-related themes to electronic devices to serve as catalytic systems or bio-organic conductive linkers.

4. Conclusion

In this study, we developed an o-CVD based synthesis pathway for the polymerization of dopamine to biopolymeric thin films. We adapted the deposition technique in order to generate PDA and demonstrate as such a versatile and simple way to form homogenous and conductive (thin-)films. Based on the spectroscopic analysis we confirm the improved C—C coupling along the polymer chain to render poly-paraphenylene backbone. The structural complexity created from the mutual reactions, intermediates and alternating monomers will continue to elucidate biopolymers in order to attain better control over the actual backbone formed. However, functional biopolymers have shown beneficial properties in particular towards bio-compatibility and stability in aqueous media. As such, we consider the design of an electrically conductive, highly functional and bio-inspired system as milestone in conductive polymers providing access to versatile linking

system between biological and organic matter by electrical signals. Among others, catalysis-related applications have targeted biopolymers - as such our simple rout to form functional synthetic polydopamine will be relevant as versatile linker at the interface of ionic and electronic systems.

Acknowledgements

Philipp Stadler is thankful to OEAD (WTZ, IN10/2015) for financial support. Niyazi Serdar Sariciftci acknowledges financial support of the Austrian Science Foundation (FWF) [Z 222-N19] within the Wittgenstein Prize Scheme.

References

[1] M. Sytnyk, E.D. Glowacki, S. Yakunin, G. Voss, W. Schofberger, D. Kriegner, J. Stangl, R. Trotta, C. Gollner, S. Tollabimazraehno, G. Romanazzi, Z. Bozkurt, M. Havlicek, N.S. Sariciftci, W. Heiss, Hydrogen-bonded organic semiconductor micro- and nanocrystals: from colloidal syntheses to (opto-)electronic devices, J. Am. Chem. Soc. 136 (2014) 16522–16532.
[2] M. Irimia-Vladu, "Green" electronics: biodegradable and biocompatible materials and devices for sustainable future, Chem. Soc. Rev. 43 (2014) 588–610.
[3] M. Irimia-Vladu, E. Glowacki, N.S. Sariciftci, S. Bauer, Small Organic Molecules on Surfaces, Springer-Verlag, Berlin Heidelberg, 2013.
[4] E.D. Glowacki, H. Coskun, M.A. Blood-Forsythe, U. Monkowius, L. Leonat, M. Grzybowski, D. Gryko, M.S. White, A. Aspuru-Guzik, N.S. Sariciftci, Hydrogen-bonded diketopyrrolopyrrole (DPP) pigments as organic semiconductors, Org. Electron. 15 (2014) 3521–3528.
[5] E.D. Glowacki, R.R. Tangorra, H. Coskun, D. Farka, A. Operamolla, Y. Kanbur, F. Milano, L. Giotta, G.M. Farinola, N.S. Sariciftci, Bioconjugation of hydrogen-bonded organic semiconductors with functional proteins, J. Mater. Chem. C 3 (2015) 6554–6564.
[6] E.D. Glowacki, G. Romanazzi, C. Yumusak, H. Coskun, U. Monkowius, G. Voss, M. Burian, R.T. Lechner, N. Demitri, G.J. Redhammer, N. Sunger, G.P. Suranna, S. Sariciftci, Epindolidiones-versatile and stable hydrogen-bonded pigments for organic field-effect transistors and light-emitting diodes, Adv. Funct. Mater. 25 (2015) 776–787.
[7] M. d'Ischia, A. Napolitano, V. Ball, C.-T. Chen, M.J. Buehler, Polydopamine and eumelanin: from structure–property relationships to a unified tailoring strategy, Acc. Chem. Res. 47 (2014) 3541–3550.
[8] D.R. Dreyer, D.J. Miller, B.D. Freeman, D.R. Paul, C.W. Bielawski, Perspectives on poly(dopamine), Chem. Sci. 4 (2013) 3796–3802.
[9] J. Liebscher, R. Mrowczynski, H.A. Scheidt, C. Filip, N.D. Hadade, R. Turcu, A. Bende, S. Beck, Structure of polydopamine: a never-ending story? Langmuir 29 (2013) 10539–10548.
[10] F. Yu, S.G. Chen, Y. Chen, H.M. Li, L. Yang, Y.Y. Chen, Y.S. Yin, Experimental and theoretical analysis of polymerization reaction process on the polydopamine membranes and its corrosion protection properties for 304 stainless steel, J. Mol. Struct. 982 (2010) 152–161.
[11] A. Huijser, A. Pezzella, V. Sundstrom, Functionality of epidermal melanin pigments: current knowledge on UV-dissipative mechanisms and research perspectives, Phys. Chem. Chem. Phys. 13 (2011) 9119–9127.
[12] P. Meredith, T. Sarna, The physical and chemical properties of eumelanin, Pigment Cell Res. 19 (2006) 572–594.
[13] A.B. Mostert, B.J. Powell, F.L. Pratt, G.R. Hanson, T. Sarna, I.R. Gentle, P. Meredith, Role of semiconductivity and ion transport in the electrical conduction of melanin, Proc. Natl. Acad. Sci. 109 (2012) 8943–8947.
[14] A.A.R. Watt, J.P. Bothma, P. Meredith, The supramolecular structure of melanin, Soft Matter 5 (2009) 3754–3760.
[15] Y.L. Liu, K.L. Ai, L.H. Lu, Polydopamine and its derivative materials: synthesis and promising applications in energy, environmental, and biomedical fields, Chem. Rev. 114 (2014) 5057–5115.
[16] Y.L. Li, M.L. Liu, C.H. Xiang, Q.J. Xie, S.Z. Yao, Electrochemical quartz crystal microbalance study on growth and property of the polymer deposit at gold electrodes during oxidation of dopamine in aqueous solutions, Thin Solid Films 497 (2006) 270–278.
[17] R.Z. Ouyang, H.P. Lei, H.X. Ju, Y.D. Xue, A molecularly imprinted copolymer designed for enantioselective recognition of glutamic acid, Adv. Funct. Mater. 17 (2007) 3223–3230.
[18] V. Ball, D. Del Frari, M. Michel, M.J. Buehler, V. Toniazzo, M.K. Singh, J. Gracio, D. Ruch, Deposition mechanism and properties of thin polydopamine films for high added value applications in surface science at the nanoscale, BioNanoSci. 2 (2012) 16–34.
[19] M.E. Lynge, R. van der Westen, A. Postma, B. Stadler, Polydopamine-a nature-inspired polymer coating for biomedical science, Nano 3 (2011) 4916–4928.
[20] A. Pezzella, A. Iadonisi, S. Valerio, L. Panzella, A. Napolitano, M. Adinolfi, M. d'Ischia, Disentangling Eumelanin "black Chromophore": visible absorption changes as signatures of oxidation state- and aggregation-dependent dynamic interactions in a model water-soluble 5,6-dihydroxyindole polymer, J. Am. Chem. Soc. 131 (2009) 15270–15275.
[21] H. Coskun, A. Aljabour, P. De Luna, D. Farka, T. Greunz, D. Stifter, M. Kus, X.L. Zheng, M. Liu, A.W. Hassel, W. Schofberger, E.H. Sargent, N.S. Sariciftci, P. Stadler, Biofunctionalized conductive polymers enable efficient CO_2 electroreduction, Sci. Adv. 3 (2017) e1700686.
[22] V. Ball, D. Del Frari, V. Toniazzo, D. Ruch, Kinetics of polydopamine film deposition as a function of pH and dopamine concentration: insights in the polydopamine deposition mechanism, J. Colloid Interface Sci. 386 (2012) 366–372.
[23] F. Bernsmann, V. Ball, F. Addiego, A. Ponche, M. Michel, J.J.D. Gracio, V. Toniazzo, D. Ruch, Dopamine-melanin film deposition depends on the used oxidant and buffer solution, Langmuir 27 (2011) 2819–2825.
[24] H. Lee, S.M. Dellatore, W.M. Miller, P.B. Messersmith, Mussel-inspired surface chemistry for multifunctional coatings, Science 318 (2007) 426–430.
[25] R.A. Zangmeister, T.A. Morris, M.J. Tarlov, Characterization of polydopamine thin films deposited at short times by autoxidation of dopamine, Langmuir 29 (2013) 8619–8628.
[26] W.J. Barreto, S. Ponzoni, P. Sassi, A. Raman, UV-Vis study of catecholamines oxidized with Mn(III), Spectrochim. Acta A 55 (1998) 65–72.
[27] J.D. Simon, Spectroscopic and dynamic studies of the epidermal chromophores trans-urocanic acid and eumelanin, Acc. Chem. Res. 33 (2000) 307–313.
[28] J.M. Gallas, M. Eisner, Fluorescence of melanin dependence upon excitation wavelength and concentration, Photochem. Photobiol. 45 (1987) 595–600.
[29] S.D. Kozikowski, L.J. Wolfram, R.R. Alfano, Fluorescence spectroscopy of Eumelanins, IEEE J. Quantum Electron. 20 (1984) 1379–1382.
[30] P. Meredith, B.J. Powell, J. Riesz, S.P. Nighswander-Rempel, M.R. Pederson, E.G. Moore, Towards structure-property-function relationships for eumelanin, Soft Matter 2 (2006) 37–44.
[31] W.C. Ye, D.A. Wang, H. Zhang, F. Zhou, W.M. Liu, Electrochemical growth of flowerlike gold nanoparticles on polydopamine modified ITO glass for SERS application, Electrochim. Acta 55 (2010) 2004–2009.
[32] A. Samokhvalov, Y. Liu, J.D. Simon, Characterization of the Fe(III)-binding site in sepia eumelanin by resonance Raman confocal microspectroscopy, Photochem. Photobiol. 80 (2004) 84–88.
[33] B. Fei, B.T. Qian, Z.Y. Yang, R.H. Wang, W.C. Liu, C.L. Mak, J.H. Xin, Coating carbon nanotubes by spontaneous oxidative polymerization of dopamine, Carbon 46 (2008) 1795–1797.
[34] A. Janotti, S.B. Zhang, S.H. Wei, C.G. Van de Walle, Effects of hydrogen on the electronic properties of dilute GaAsN alloys, Phys. Rev. Lett. 89 (2002) 086403.
[35] M.D. Shultz, J.U. Reveles, S.N. Khanna, E.E. Carpenter, Reactive nature of dopamine as a surface functionalization agent in iron oxide nanoparticles, J. Am. Chem. Soc. 129 (2007) 2482–2487.
[36] J. Mcginness, P. Corry, P. Proctor, Amorphous-semiconductor switching in melanins, Science 183 (1974) 853–855.
[37] J.E. McGinness, Mobility gaps: a mechanism for band gaps in melanins, Science 177 (1972) 896–897.